CHAPTER II

DIODES

2.1 INTRODUCTION

The forward ON voltage, reverse blocking voltage and reverse recovery time are three important characteristics of a diode. The forward ON state voltage is required to be the lowest possible for low power dissipation, breakdown voltage the highest possible depending upon targeted application and reverse recovery time should be the least possible for faster switching. While improving the reverse recovery of the diode by the incorporation of “universal contact” (UC) no deleterious effects on the ON state voltage and breakdown voltage are desired. Keeping this in view, a brief review of these characteristics and their dependence on diode parameters is taken up before going to analysis and modeling of the effects caused by the incorporation of the UC.

The ON state voltage is comprised of built-in voltages at both diffused junctions and voltage drop in middle region. The ON state characteristics [16] of an ideal diode can be described by the relationship

$$J = \frac{4 q D_a n_i}{W_M} F\left(\frac{W_M}{2L_a}\right) e^{\left(\frac{qV_A}{kT}\right)} \qquad (2.1)$$

Where V_A is the applied voltage, W_M is the width of the drift region, L_a is the ambipolar diffusion length and $F\left(\frac{W_M}{2L_a}\right)$ is a function given as under

$$F\left(\frac{W_M}{2L_a}\right)=\frac{\left[\left(\frac{W_M}{2L_a}\right)\tanh\left(\frac{W_M}{2L_a}\right)\right]}{\sqrt{1-\frac{1}{4}\tanh^4\left(\frac{W_M}{2L_a}\right)}}e^{-\left(\frac{qV_M}{2kT}\right)} \qquad 2.1(a)$$

Where V_M, is the voltage drop in the middle region. As seen from Fig. 2.1, the function $F\left(\frac{W_M}{2L_a}\right)$ is maximum when half of the drift region width ($\frac{W_M}{2}$) is equal to the diffusion length, L_a. Thus, as the speed of the rectifiers is increased through the lifetime reduction while keeping the W_M constant, it would be accompanied by deterioration in

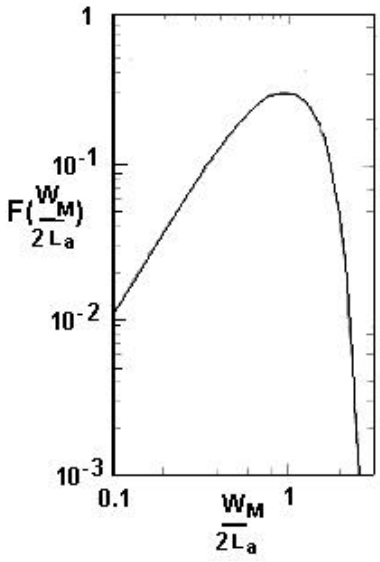

Fig. 2.1 Function F ($W_M/2L_a$)

the forward ON voltage if initially the design is optimal ($W_M = 2\ L_a$). This illustrates an important trade off that exists between the switching speed and the forward voltage drop in the design of the power diode. The current and related voltage drops have been extensively studied [17-20].

The doping and the width, W_M of the drift region determines the breakdown voltage of the diode. For better forward characteristics, lower W_M is desirable as seen from Eq. (2.1). As the forward current density is independent of the background doping, the width is optimized to be minimum by lowering the background doping for a given breakdown voltage. The power diodes are usually made of punch-through type i.e. their width; W_M is less than the depletion width at the avalanche breakdown. The punch through voltage, V_{PT} for a parallel plane junction is given by

$$V_{PT} = E_C W_M - \frac{q N_D W_M^2}{2 e_s} \qquad (2.2)$$

The critical electric field is a weak but increasing function of doping [21] and increases with increase in doping. Taking this variation in the critical electric field into consideration, an optimum width and doping can be found out for parallel plane junction.

The junctions are usually made by diffusion using oxide masks. This process results in spherical and cylindrical junctions at corners and edges respectively. Due to this reason, the actual breakdown voltage in planar junctions is about 50% of the parallel plane junction. At high voltage the curved junction give rise to high fields near the surface and this induces ionic instability at the surface which causes increased leakage

and soft breakdown. As a result, the curved portions are chemically etched out and passivated in high (>500 V) voltage devices. One of the methods to remove curved portion is the mesa etching. The etched portion is then filled with glass to passivate the junction. The actual breakdown voltage is restored to 80% of the parallel plane junction. The effect of edge termination technique upon the breakdown voltage and its relationship with the width and doping of the drift region has been summarized in Table 'A'. In high voltage diodes the doping of the drift region is low and width is large. Due to the low doping of the drift region, lifetime in the diode is high and this degrades the reverse recovery.

The reverse recovery time depends on the total charge stored in the diode in the ON state. A high lifetime in the middle drift region leads to large minority charge storage in the diode. Further, the structure of the conventional diode keeps the minority charge confined to the large drift region. Generally, the diode has a p^+-υ-n^+ type of structure as shown in Fig. 2.2(a). In high voltage diodes, p^+ and n^+ are diffused in a bulk wafer. Low voltage diodes are typically made by p^+ diffusion in n on n^+ epitaxial wafer. The diffused regions give rise to electric fields due to the concentration gradient [22]:

$$E = \frac{kT}{q}\frac{1}{N}\frac{dN}{dx} \qquad (2.3)$$

This electric field is also evident in the band diagram shown in Fig. 2.2(b). In the ON state, the electric field opposes the transport of minority carriers across the diffused regions. The injected electrons in left p-diffused region face opposing electric field due to this concentration gradient and similarly, the holes also face opposing electric field in the

right n-diffused region. In case of n-n^+ epitaxial interface, the dN/dx gradient is very sharp and opposition to minority carriers greater and consequently there is little penetration of minority carriers across this layer. This results in the minority charge being confined to the middle drift region. When the device is turned off, the current continues to flow in the device till all the minority charge is removed. This effect gives rise to long reverse recovery which consists of constant reverse current phase called storage time and 90% of the fall time delay.

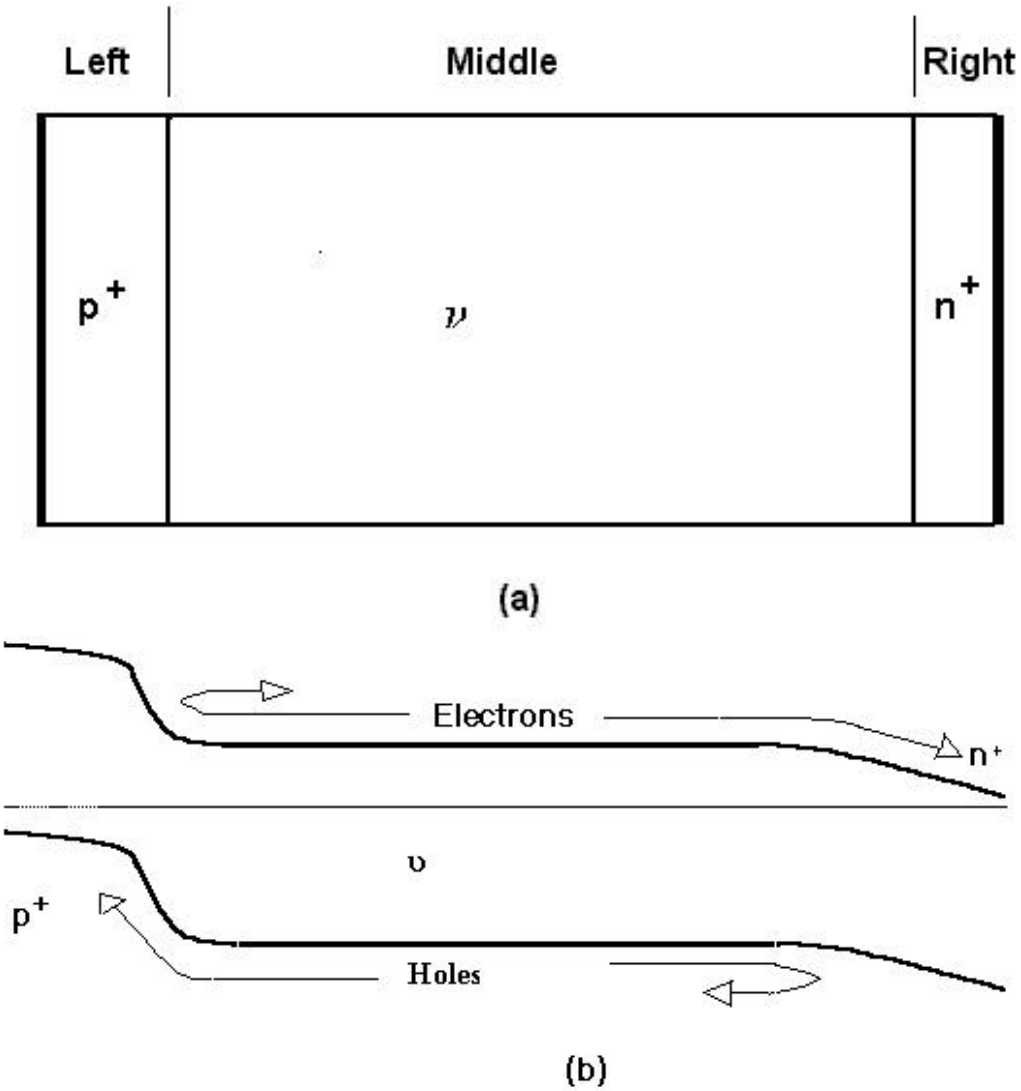

Fig. 2.2 (a) Conventional diode structure (S-I) and its (b) Band diagram with carrier flow directions

2.2 DIODE STRUCTURE (S-II) TO REDUCE THE REVERSE RECOVERY AND TO DECREASE 'ON' STATE VOLTAGE

In conventional diode structures shown in Fig. 2.2(a) most of the minority charge is stored in the lightly doped υ region. The holes that are injected into this region are confined by the reflecting υn$^+$ contact as explained earlier. In the device proposed by Amemiya [2] et al shown in Fig. 2.3, henceforth referred to as structure S-II, an additional path for exit of holes from the lightly doped region has been provided through incorporation of the p$^+$ diffusion in a mosaic pattern alternate with n$^+$ diffusion. The n$^+$p$^+$ when connected with a common metal form an equi-potential contact, called "universal contact" (UC) as it is truly ohmic for both electrons and holes. It has been shown [2] that the introduction of universal contact leads to significant reduction in reverse recovery time and also lowering of the 'ON' state voltage.

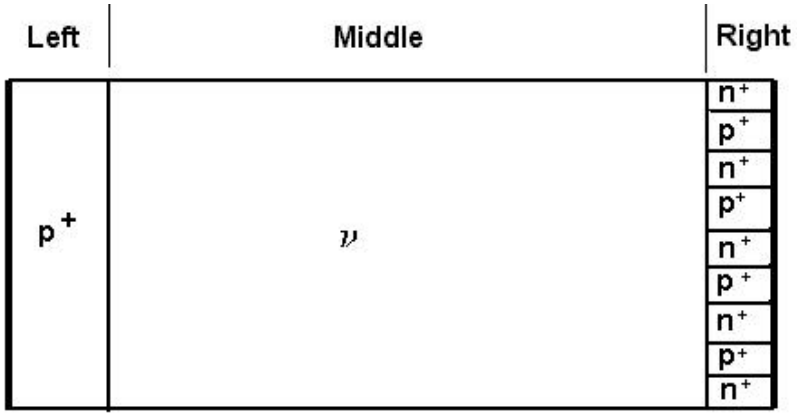

Fig. 2.3 Diode incorporating "universal contact" (S-II)

Though, there is significant improvement in reverse recovery by incorporating the universal contact as done in Amemiya structure Fig. 2.3, this approach cannot be applied to conventional high voltage diode structures due to the following reasons.

1. To isolate the devices, grooves have to be formed around the edge of each device extending to interface between the ν-type epitaxial layer and the p+ substrate to create individual diode [23]. This can easily be done for thin epiaxial layer. For high voltage diode made in epitaxial wafers of 50 – 100 μm epi-layer or in bulk devices, it is not convenient.

2. The diode structure as shown in Fig. 2.3 in effect becomes a $p^+\upsilon p^+$ side by side the $p^+\upsilon n^+$ due to the extension of p^+ diffused region for making the universal contact up to the edge of the nn^+ interface. In low voltage diodes, the doping of the drift region is comparatively high. On application of reverse bias, depletion layer starting from the $p^+\upsilon$ junction do not extend to the back p^+n^+ universal contact before the reverse avalanche breakdown takes place. In high voltage diodes though the drift region width is large, the depletion layer quickly extend to other end on application of high reverse bias due to the inverse quadratic depends of depletion layer on drift region doping. As seen from the Table 'A', the doping of the drift region of high voltage diode is approximately two orders of magnitude smaller in comparison to low voltage diodes. This results in the extension of the depletion layer to the edge of p^+n^+ universal

contact, which causes reach through reverse breakdown. This reach through breakdown is different from the reverse breakdown in the $p^+ \nu n^+$ punch-through diodes discussed in the last section. In the punch-through diode, the phenomenon of avalanche multiplication due to the high electric field causes reverse breakdown. The reach through breakdown of $p^+ \nu p^+$ high voltage diode structure incorporating universal contact (S-II) takes place at a much lower voltage in comparison to avalanche breakdown.

2.3 MODIFIED DIODE STRUCTURE (S-III)

To avoid the above problems, a diode structure shown in Fig. 2.4, henceforth called the diode structure S-III has been proposed by Kitagawa [13]. The important feature of the S-III is that the UC has been incorporated within the diffused region away from the junction. In reverse mode, most of the depletion layer extends into low-doped ν region. The diffused p^+ region inhibits depletion layer extending into it and thus avoids punch-through. It is shown that the reverse recovery and forward ON voltage in S-III are smaller than in S-I. As seen above, the original concept of universal contact has been suitably modified for high voltage diodes to realize a shorter reverse recovery and low ON state voltage. With the coming up of the new applications for faster switching, further understanding of the mechanisms of reduction of reverse recovery by the incorporation of UC is desirable.

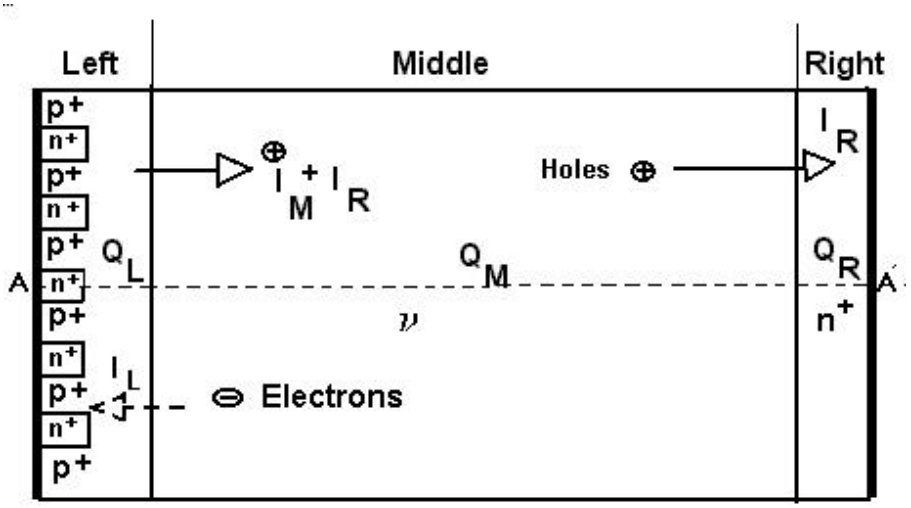

Fig. 2.4 Modified diode structure (S-III)

Keeping this in mind, efforts have been made in next sections to analyze and model the effect of charge storage, current conduction in diode and the effect of the incorporation of UC in diode on reverse recovery and other important characteristics.

2.4 MODELLING & SIMULATION OF EFFECTIVE LIFETIME

The improvement in switching delay obtained through incorporation of universal contact in S-II and S-III can be viewed from another angle, aside from the mechanism of providing another path for exit of carriers from the lightly doped region. The switching delay is closely related to the effective minority carrier lifetime in the device defined as

$$t_{eff} = \frac{Q}{I} \qquad (2.4)$$

Where Q is the total minority charge stored and I, is the total current flowing through the diode. Fig. 2.5 shows a comparison of the effective lifetime for a conventional diode structure, S-I along with the total reverse recovery time as a function of current density. These results were obtained through 2D numerical simulation using the Silvaco device simulation package [15] for a diode of breakdown voltage of 1000 Volts. The description of the diode is given in Table 2.1.

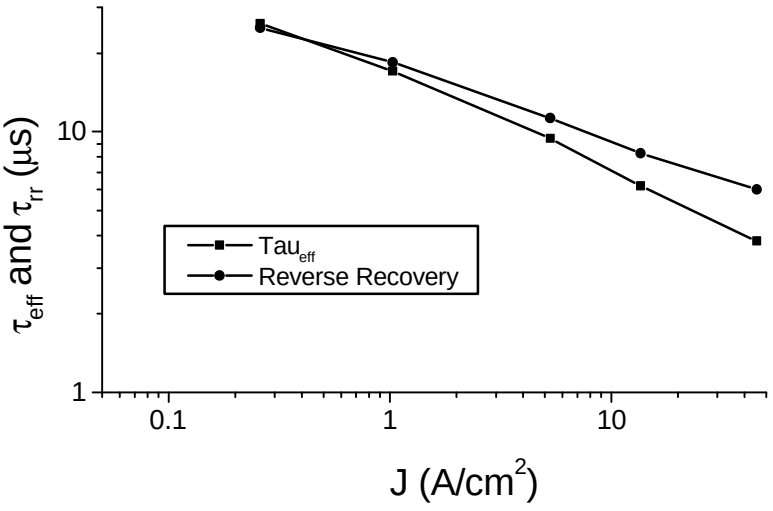

Fig. 2.5 Comparison of reverse recovery (t_{rr}) and effective lifetime (t_{eff}) as a function of current density for high voltage diode (S-I)

The 2D simulations are based on drift-diffusion formalism and take into account the concentration dependent SRH recombination, concentration and field dependent mobility, band gap narrowing and Auger effects. The reverse recovery time is defined as the total time for which the diode conducts in the reverse direction and is the sum of

storage and fall times. It can be seen from the figure that the effective minority carrier lifetime tracks total reverse recovery time quite well. Although, reverse recovery waveform can be quite complicated with several distinct regions such as storage time, fall time etc, for ease of analysis, the subsequent discussion will deal primarily with the effective lifetime.

The current I in Eq. (2.4) can be divided into three components [24], the minority electron current injected into the left region I_L, hole recombination current I_M, in the middle region and hole current I_R injected into the right region. Similarly, the minority charge Q, can be considered as having three components Q_L, Q_M and Q_R in the left, middle and right regions respectively. With these definitions, t_{eff} may be re-written as

$$t_{eff} = \frac{t_M \bullet \left(1 + \frac{Q_L}{Q_M} + \frac{Q_R}{Q_M}\right)}{\left(1 + \frac{I_L}{I_M} + \frac{I_R}{I_M}\right)} \qquad (2.5)$$

Where $t_M = \frac{Q_M}{I_M}$ is high-level injection lifetime in the lightly doped middle region.

It is a fairly good assumption that the minority charges Q_L, Q_R in the p and n-regions are much smaller than the minority charge Q_M in the middle region because the doping in left and right regions are much larger as compared to that in the middle region.

However, the currents injected into the left and right regions are not negligible so that the Eq. (2.5) can be simplified to

$$t_{eff} = \frac{t_M}{\left(1+\frac{I_L}{I_M}+\frac{I_R}{I_M}\right)} \qquad (2.6)$$

Eq. (2.6) can be re-written in an alternative form as

$$\frac{1}{t_{eff}} = \frac{1}{t_L} + \frac{1}{t_M} + \frac{1}{t_R} \qquad (2.7)$$

Where $t_L = t_M I_M/I_L$ and $t_R = t_M I_M/I_R$.

Eq. (2.7) shows that the effective minority carrier lifetime in the diode is a function of three time constants and only one of which is the recombination lifetime in the lightly doped middle region. The conventional approach for improving reverse recovery, under the tacit assumption $t_{eff} \cong t_M$, have accordingly focussed attention on reducing this lifetime through incorporation of impurities such as Au, Pt etc. Eq. (2.7) however, suggests other alternative techniques for reducing the effective minority carrier lifetime by reducing other time constants such as t_L or t_R. The expressions for these time constants show that this would require an increase of either the I_L/I_M or the I_R/I_M current ratios. The reason for this improvement is that while a thick, lightly doped middle region is well suited for the task of reverse blocking, it is unsuitable for carrying a

substantial share of minority carrier current due to high recombination lifetime. On the other hand, the heavily doped n^+ and p^+ regions of the diodes, are better suited to carry a larger fraction of minority carrier current because of lower recombination lifetimes in these regions. Accordingly, as indicated by Eq. (2.6), it makes sense to divert minority carrier current away from the lightly doped middle region to other regions of the diode where lifetime is lower. This principle, of diverting current away from regions of high recombination lifetime to regions of low recombination lifetime is well known and applied for example in BJTs, where sometimes a Schottky diode is connected across the collector-base junction so as to improve the transistor's switching performance. In this case a large fraction of the base current in saturation is diverted from the collector-base junction of the transistor, where minority carrier lifetime is high, to Schottky diode, which is characterized by negligible minority carrier storage. The use of universal contact provides a mechanism for implementing this principle within PIN diodes as explained in detail below.

Let us consider how the ratio I_L/I_M can be increased so as to reduce the effective recombination lifetime. The current I_L results from injection of electrons into the p-diffused left region. These electrons are normally reflected back by the sharply increasing p-type doping profile, thus limiting the minority carrier current I_L to a small value. However, if a "universal contact" is incorporated in the diffused region, the minority carrier current I_L can be significantly increased. This contact should however be inserted so that, there is no reach-through prior to avalanche breakdown when the diode is in the reverse blocking state. This can be done by restricting the depth of n^+ diffusion to less than the extent of the depletion layer at the breakdown voltage. This structure is expected

to result in improvement in switching performance but without any decrease in reverse breakdown voltage.

To verify the above concept, the diodes S-I and S-III were studied through 2D numerical simulations. The details of the structure of the diodes are listed in Table 2.1. Both, the diodes are designed for a breakdown voltage of ~150 Volts.

Table 2.1 - Details of the Simulated Diodes

Diodes	Base Resistivity/ Doping and Width	n^+ substrate/ Right side N^+ diffused Region thickness and doping	p diffusion	p^+ diffusion for making "universal contact"	n^+ diffusion in p for "universal contact" (Refer Fig.2.4)
(1)Low Voltage (S-1 & S-III) (~ 150 V)	nn^+ epi, n width 15 µm & Conc.1.15 x 10^{15} /cm^3.	n^+ substrate thickness 300 mm, Doping > 10^{20}/cm^3.	Xj=5.7 mm, Surface Conc. 2 x 10^{18}	Xj=1.6 mm, Surface Con 2.0 x 10^{19}	Xj=3.0 mm, Surface Con. 4.0 x 10^{20}
(2)High Voltage (S-1 & S-III) >1000 V)	4 x 10^{13} /cm^3, 140 mm Bulk silicon,	n^+ Right side diffused region thickness 35 mm, Surface con. ~ 4x10^{18} /cm^3.	Xj=22 mm, Surface Conc. 7 x 10^{17}	Xj=2.2 mm, Surface Con 5.0 x 10^{19}	Xj=4.1 mm, Surface Con. 8 x 10^{19}

Fig. 2.6 shows a comparison of the effective lifetime obtained for the low voltage diodes S-I and S-III. The effective lifetime decreases from 849 ns to 194 ns, a reduction of 77% at 1 A/cm^2 and from 88 ns to 28 ns a reduction of 68% at about 110 A/cm^2.

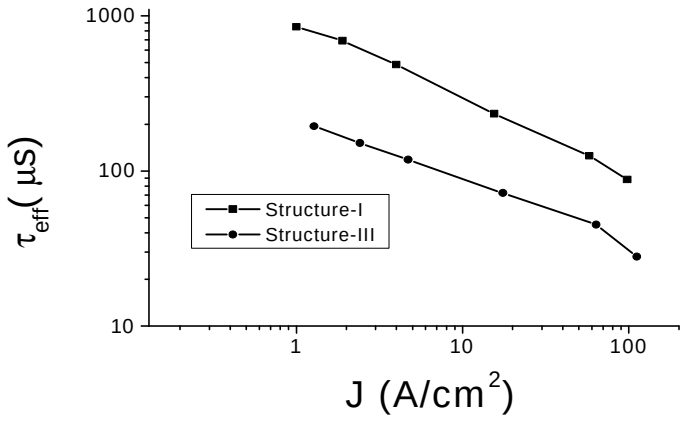

Fig. 2.6 t_{eff} vs J for low voltage diodes (S-I & III)

The improvement in effective lifetime obtained was found to be similar to the improvement observed in reverse recovery under both hard and soft switching conditions indicating that effective minority carrier lifetime is a good and simple measure of the switching performance of the diode.

Fig. 2.7 shows a comparison of effective lifetime of the two structures designed for reverse blocking voltage of around 1000 V. In these high voltage diodes, t_{eff} decreases from 26 ms to 15.4 ms, a reduction of 41% at 0.3 A/cm^2 and from 3.8 ms to 2.3 ms, a reduction of 39% at about 50 A/cm^2.

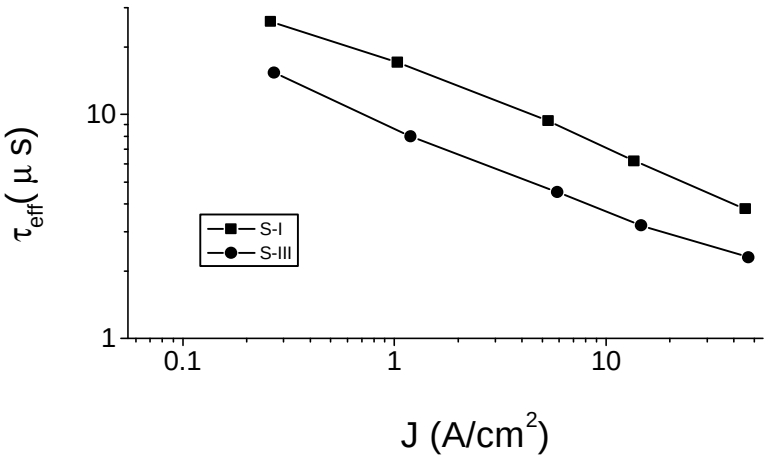

Fig. 2.7 t_{eff} vs J for high voltage diode (S-I & III)

These results can be explained in terms of changes in the current ratio I_L/I_M. Figs. 2.8 and 2.9 show a comparison of the ratio I_L/I_M for the low and high voltage diodes respectively.

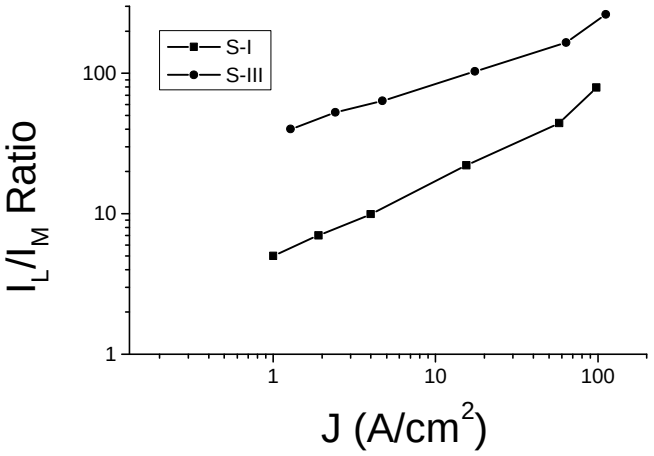

Fig. 2.8 **I_L/I_M ratio for low voltage diodes (S-I & III)**

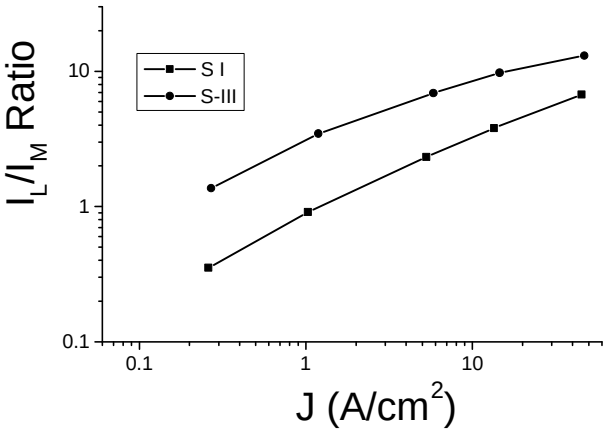

Fig. 2.9 **I_L/I_M ratio for high voltage diodes (S-I & III)**

The reduction of reverse recovery time by 77% for the low voltage case can be largely attributed to an increase of the ratio I_L/I_M, from 5 to 38.6. Similarly, the results for high voltage diode can be attributed to improvement in the I_L/I_M ratio.

Fig. 2.10 (a) and (b) shows the two representative simulated reverse recovery waveforms under hard and soft reverse recovery respectively using resistive load. The forward voltage is 4.7 V and reverse voltage is 3.5 V. In Fig. 2.10 (b), the voltage is ramped from forward voltage to reverse peak voltage in 10 μs. In step recovery; the same was done in 2 ns. The effective lifetimes as obtained either from hard or soft recovery is same.

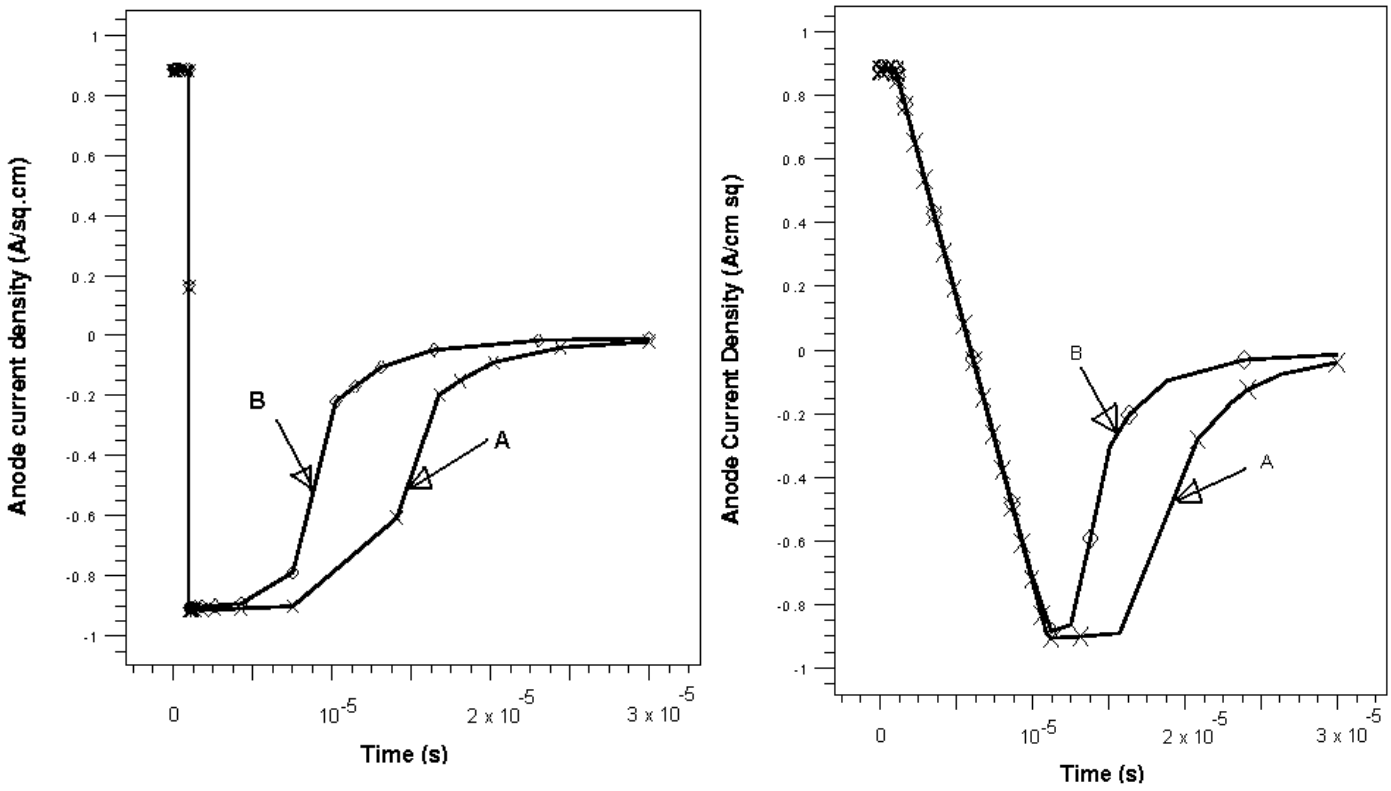

(a) **(b)**

Fig. 2.10 **Simulated current waveform under (a) hard/step Recovery (b) soft/ramp Recovery**
(Waveform marked 'A' is for diode S-I and 'B' for diode S-III)

2.5 MODELING & SIMULATION OF DEPENDENCE OF END CURRENTS ON DEVICE PARAMETERS

The variation of the current ratio I_L/I_M with current density and also the difference in effective lifetime between the low and high voltage diodes can be explained using a simple analytical model. Fig. 2.11 shows a 1D view of the device in the region where n^+ diffusion in p-diffused region has been made. The $x_{j1,}$ x_{j2} and x_{j3} are the metallurgical

junctions of front n^+p "universal contact", pυ diode and back $υn^+$ contact. The x_1 and x_2 are the depletion edges of n^+p and pυ junctions inside the p diffused region.

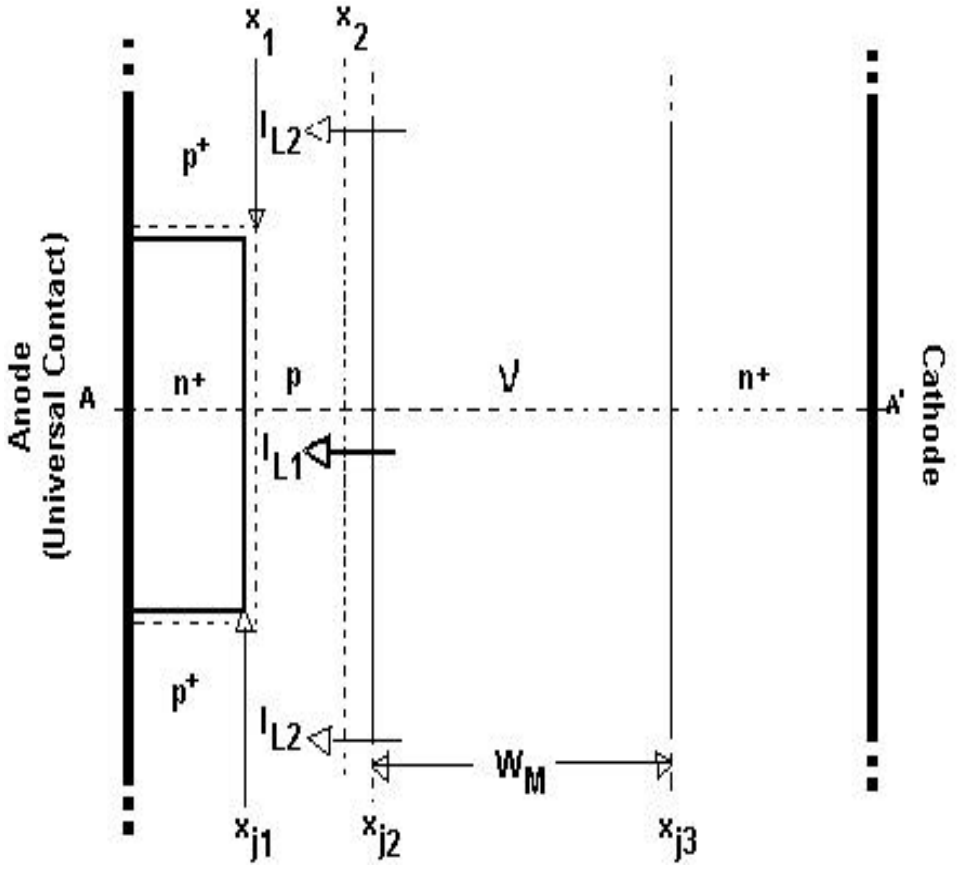

Fig. 2.11 One dimensional diode structure under n^+ (At cross - section A-A') of Fig. 2.4

Since the current ratio I_L/I_M is the most important factor affecting the minority carrier lifetime, let us look at some of the important factors that influence this ratio. The current injected into the left region can be divided into two components: a component, I_{L1}

flowing under n^+ and other component, I_{L2} under p^+. Since $I_{L1} >> I_{L2}$, $I_L \approx I_{L1}$. Under steady forward bias conditions, the current density I_L due to electron flow in the left p-diffused region can be written [25] as

$$I_L = \frac{q^2 n_i^2 D_n \exp\left(\frac{qV_L}{kT}\right)}{Q_p} x_L A \qquad (2.8)$$

Where A is the area of the diode and ξ_L is the fraction of the area in which n^+ has been introduced. Defining a factor $\eta_L = \frac{V_A}{V_L}$, where V_A is the applied voltage, equation (2.8) may be written as

$$I_L = q^2 n_i^2 D_n A \frac{\exp\left(\frac{qV_A}{h_L kT}\right)}{Q_p} x_L \qquad (2.9)$$

For simplicity, we assume that when junction is forward biased $x_2 = x_{j2}$ and low level injection conditions prevail so that $Q_p = q\int_{x_1}^{x_{j2}} N_a(x)\,dx$. To avoid reach-through prior to onset of avalanche breakdown, we require that at breakdown $(xj_2 - x_1) > 0$. Taking E_C as the critical field, we obtain the condition

$$\frac{q}{e_s}\int_{x_1}^{x_{j2}} N_a dx > E_C \qquad (2.10)$$
$$or\ Q_p > e_s E_C$$

Defining $f_L = \frac{Q_p}{e_S E_C}$, allows Eq. (2.9) to be re-written as

$$I_L = q^2 n_i^2 D_n A \frac{\exp\left(\frac{qV_A}{h_L kT}\right)}{f_L e_s E_C} x_L \qquad (2.11)$$

The factor f_L represents a safety factor in the sense that for f_L > 1, the charge, Q_p under the universal contact is large enough to prevent onset of reach-through prior to onset of avalanche breakdown. On the other hand if f_L < 1, then the reverse blocking voltage would be determined primarily by the occurrence of reach-through.

The middle region current, I_M is the minority carrier current and can be modeled as recombination current [17], which may be written as

$$I_M = qn_i A \frac{W_m}{t_M} \exp\left(\frac{qV_A}{h_M kT}\right) \qquad (2.12)$$

Where h_M is the ideality factor of the current, I_M. The ratio I_L/I_M can now be obtained using Eq. (2.11) and Eq. (2.12) as

$$\frac{I_L}{I_M} = q\, n_i D_n \frac{t_M}{W_M} \frac{\exp\left(\frac{qV_A}{kT}\left(\frac{1}{h_L} - \frac{1}{h_M}\right)\right)}{f_L e_s E_C} x_L \qquad (2.13)$$

The total current density J of the diode may be written in terms of its ideality factor n as

$$J = J_O \exp\left(\frac{qV_A}{nkT}\right) \qquad (2.14)$$

Equation (2.14) can be used to re-write Eq. (2.13) as

$$\frac{I_L}{I_M} = C_L \frac{t_M}{W_M} \frac{J^{a_L}}{f_L} x_L \qquad (2.15)$$

Where $a_L = n \times \frac{h_M - h_L}{h_M h_L}$ and constant factor, $C_L = \frac{q\, n_i\, D_n}{e_s E_C\, J_0^{a_L}}$

Substitution of Eq. (2.15) in Eq. (2.7) and neglecting the ratio I_R/I_M that is smaller than the ratio I_L/I_M, we obtain

$$\frac{1}{t_{eff}} \cong \frac{1}{t_M} + \frac{1}{t_L} \qquad (2.16)$$

Where $t_L^{-1} = C_L \frac{J^{a_L}}{f_L W_M} x_L$

Equation (2.16) predicts that the effective lifetime will decrease with increase in current density. This is due to the different ideality factors of the current injected into the middle and the left regions of the diode. A plot of the ideality factors for three different current components as extracted from simulations using Eq. (2.17) of diode S-I is shown in Fig. 2.12.

$$h = \frac{q}{kT} \Delta V \ln\left(\frac{J_2}{J_1}\right) \qquad (2.17)$$

DV is the change in applied voltage when the current density is varied from J_1 to J_2. The value of η_M is ~2 and that of η_L and η_R is ~1.

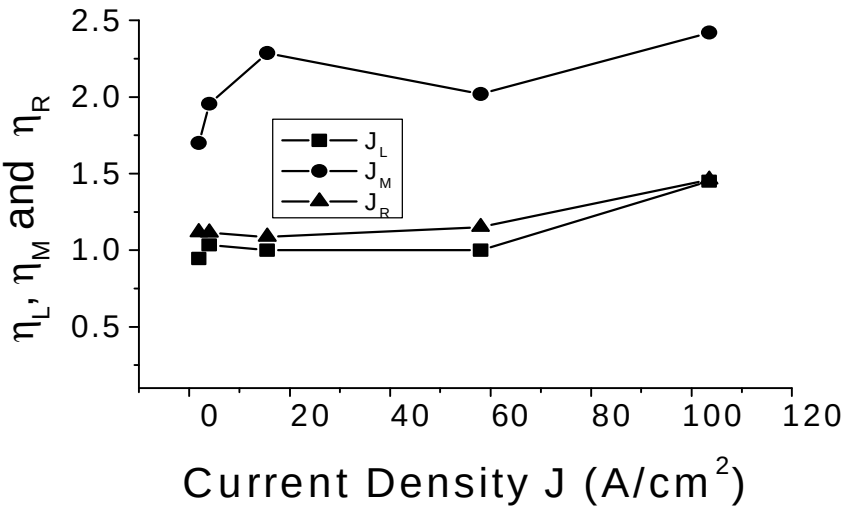

Fig. 2.12 - J vs Ideality Factor for end region currents and middle region current for low voltage diode (S-I)

The minority hole current in the middle region increases as $\exp\left(\frac{qV_A}{2kT}\right)$ due to high level injection in the middle region, while the current injected into the left region increases as $\exp\left(\frac{qV_A}{kT}\right)$ due to low level injection condition, causing the ratio I_L/I_M to increase with increase in bias or the time constant τ_L to decrease with increase in current density.

Eq. (2.16) also shows that the impact of insertion of universal contact on effective lifetime will decrease as the breakdown voltage of the diode increases. This is because; increase of breakdown voltage requires increase of the thickness W_M of the lightly doped middle region, which increases the time constant τ_L. Thus, like the conventional PIN

diode, in this case also, there is a tradeoff between the reverse recovery and the reverse blocking voltage.

Instead of the left p^+ region, the universal contact can also be inserted in the right n^+ region. For this case, an expression similar to Eq. (2.16) can be written

$$\frac{1}{t_{eff}} \cong \frac{1}{t_M} + \frac{1}{t_R} \tag{2.18}$$

Where $t_R^{-1} = C_R \frac{J^{a_R}}{f_R W_M} x_R$

Both Eq. (2.16) as well as Eq. (2.18) shows that a decrease in safety factors can result in improvement in the effective lifetime. In fact, f_R may be made even less than unity by inserting the universal contact deeper into the n^+ region. In this case the reverse blocking voltage would be compromised due to onset of reach-through prior to avalanche breakdown. This illustrates that the reverse blocking characteristics can be traded with the switching characteristics in a new manner determined by the proximity of the universal contact to the edge of the lightly doped region. This is exactly what is done in the structure S-II proposed by Amemiya et al, where the universal contact is inserted in the right n^+-region of the diode such that it is contiguous with the middle region. Although Eq. (2.18) ceases to hold when f_R becomes zero, we expect that a large decrease in effective lifetime would result at the expense of a drop in the reverse blocking voltage especially in diodes designed for high voltage operation. This is illustrated in Fig.

2.13 where the structures S-I and S-II are compared. As can be seen, the effective lifetime is significantly reduced in diode S-II in comparison to conventional diode S-I.

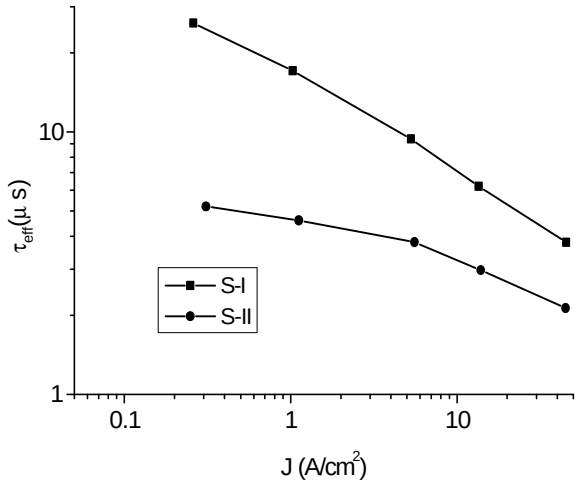

Fig. 2.13 t_{eff} vs J of high voltage diode (S-I and S-II)

Fig. 2.14 shows a comparison of the ratio I_R /I_M for the two structures, S-I and S-II. The increase in this current ratio for S-II completely accounts for its better performance.

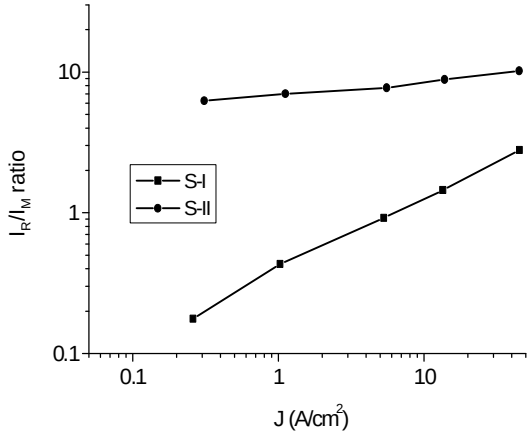

Fig. 2.14 I_R/I_M for high voltage diode (S-I & II)

The simulated reverse characteristics of diode S-I and S-II are shown in Fig. 2.15. It can be seen that the diode S-II suffers from premature breakdown due to reach-through between the two p^+ regions, one on the left and the other on the right side.

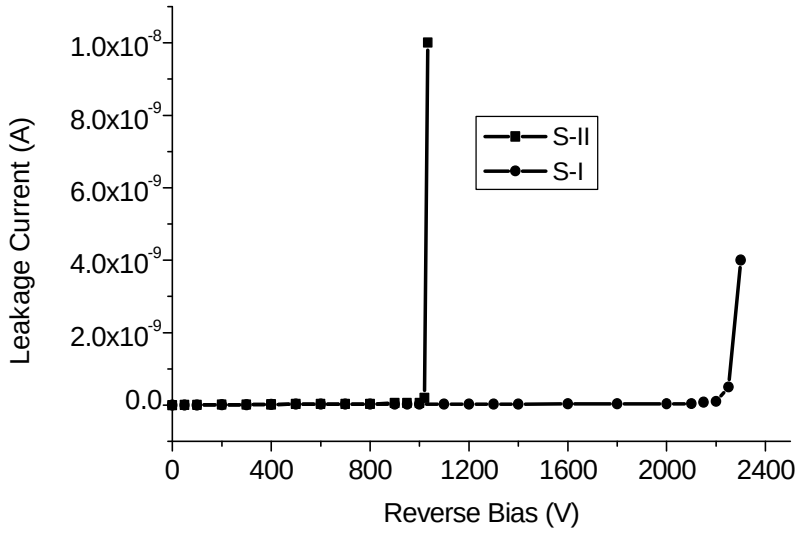

Fig. 2.15 Simulated breakdown voltage of diodes (S-I & II)

The onset of this p^+-n-p^+ reach-through in S-II limits the reverse blocking voltage to less than half the breakdown voltage of the conventional diode S-1. This reach-through phenomenon is either absent or less severe in low voltage diodes because the doping in the middle region is relatively high and as a result, the depletion layer on application of reverse bias does not reach the p^+ region even at breakdown voltage.

During reverse recovery, the reverse current consisting of holes flows only through the p^+ part of the universal contact. This results in lateral current flow and voltage drop under the n^+ regions of the universal contact as illustrated in Fig. 2.16, which may result in turn-on of the parasitic n^+pvn^+ transistor [26]. To determine whether this is likely to happen or not, let us try to estimate the lateral voltage drop at current densities of interest. Taking the approximation that the current flows in lateral x direction under n^+, this may be analyzed by taking a single n^+ diffusion of width, L inside p^+ region as shown in Fig. 2.16.

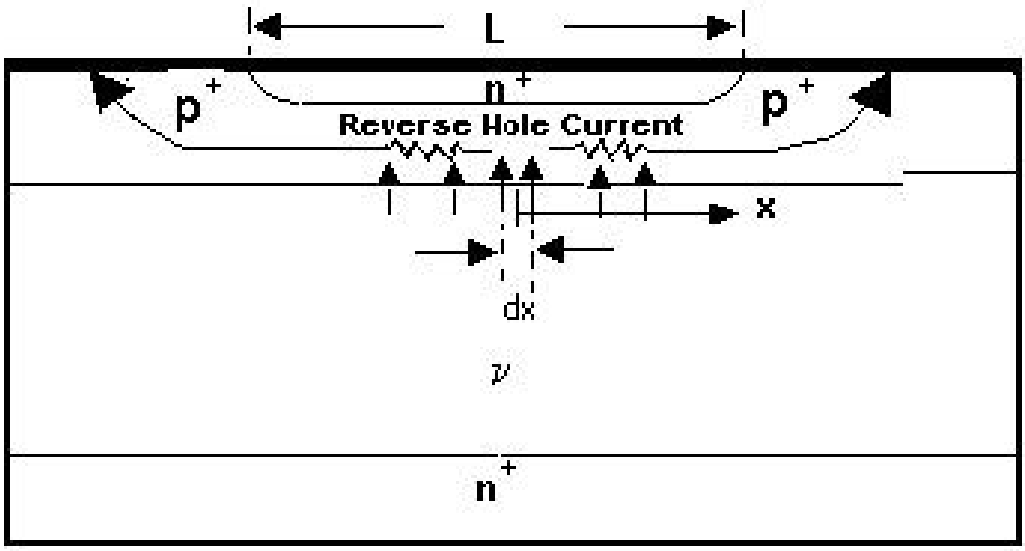

Fig. 2.16 Universal contact region showing flow of current under n^+ in reverse bias condition

Taking x = 0 at the center of n^+ finger, the current under n^+ may be written as

$$I(x) = \int_0^x J_z \, dx = J_z \, x \qquad (2.19)$$

Where z is the dimension perpendicular to the plane of the paper.

$$dV(x) = I(x) \quad \frac{r_S}{z} dx \qquad (2.20)$$

Where ρ_S is the sheet resistance of the diffused region and dV is the small voltage drop across small distance dx.

$$V = \int_0^{L/2} dV_{(x)} dx = J \rho_S \int_0^{L/2} x\, dx \qquad (2.21)$$

$$= J \rho_S \quad \frac{L^2}{4}$$

Assuming that V = 0.7 V is required to turn on the parasitic NPN transistor, the width of the n^+ contact for which the parasitic transistor may turn ON has been calculated as a function of current density and is given for few current density values.

For 100 A/cm^2, L= 167 μm;

For 500 A/cm^2, L= 74.8 μm;

For 1000 A/cm^2, L= 52.9 μm;

ρ_S = 100 Ω/sq. has been assumed.

These results indicate that for a width of 60 μm, there is no possibility of turn-on of the parasitic transistor. These results were confirmed through simulation and it was found through that for n^+ : p^+:: 60 μm : 40 μm, the voltage difference under p^+ and n^+ is

only a few mV and turn-on of the parasitic transistor has not been observed even under hard reverse recovery.

2.6 A Proposed Diode Structure

The improvement in effective minority carrier lifetime would be maximum when "universal contact" is incorporated in both the left p^+ and the right n^+ regions as illustrated in Fig. 2.17, henceforth referred to as diode S-IV. By keeping the safety factors larger than unity, the new structure is expected to give significant improvement in effective lifetime without compromising the reverse blocking voltage.

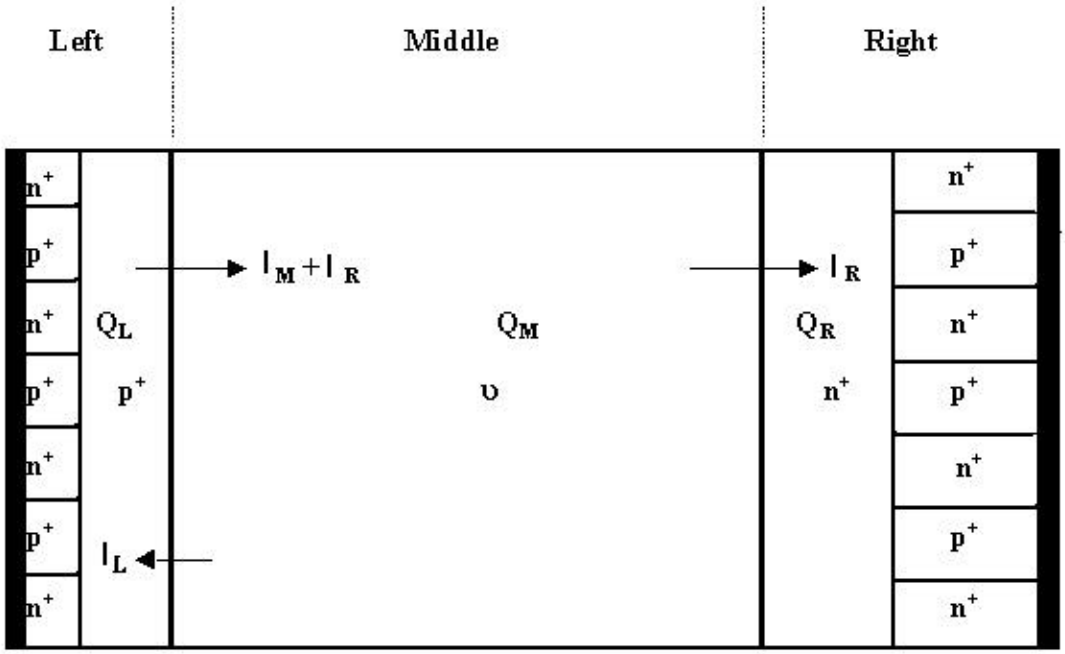

Fig. 2.17 A proposed diode structure (S-IV)

A comparison of effective lifetimes for the structures S-I, II, III and IV is shown in Fig. 2.18 for a diode designed for reverse blocking voltage of >1000 Volts.

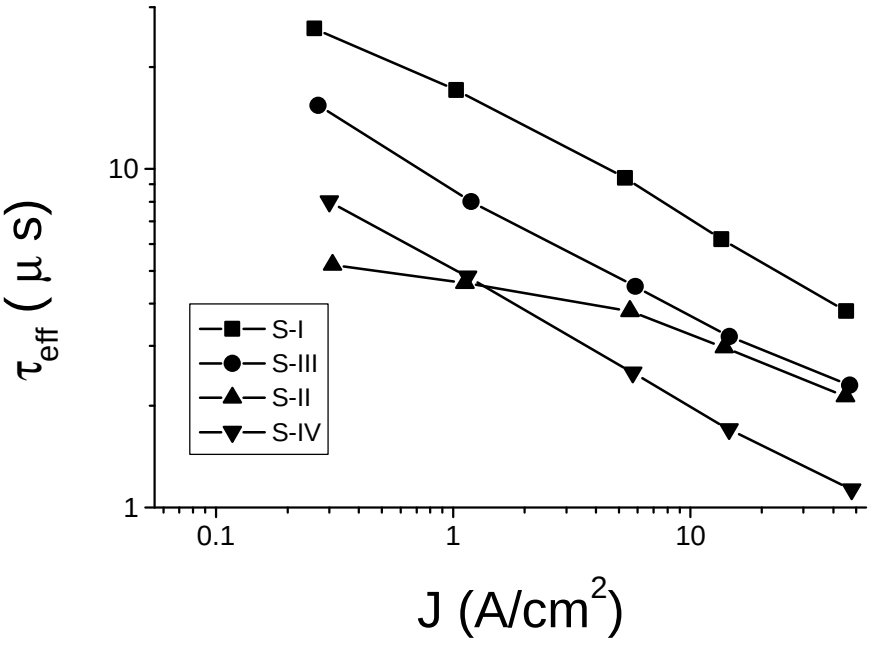

Fig. 2.18 A comparison of t_{eff} vs J of diodes (S-I, II, III & IV)

As expected, the new structure S-IV shows better effective lifetime than that of diode S-I and diode S-III. It also compares well with diode S-II, particularly at higher current density. Fig. 2.19 and 2.20 show a comparison of current ratios I_L/I_M and I_R/I_M for the different diodes S-I to IV. The improvements in reverse recovery are 60% and 66% at low and high current densities respectively in the proposed structure with respect to conventional structure. The corresponding values of reverse recovery improvement in diode S-II are 74% and 40%. The better performance of the new structure S-IV can be attributed to improved values for both I_L/I_M and I_R/I_M ratios in the device.

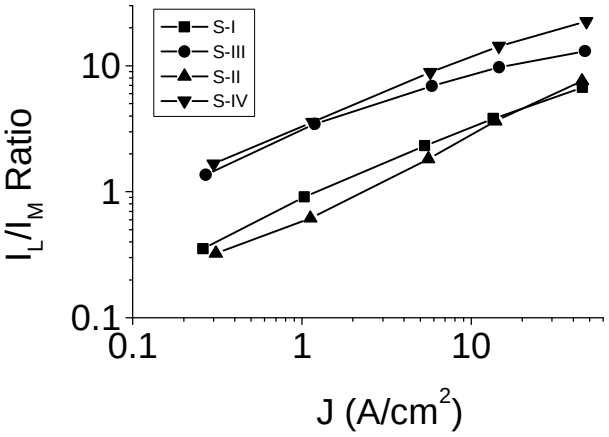

Fig. 2.19 - A comparison of I_L/I_M of diodes S-I , S-II, S-III and S-IV

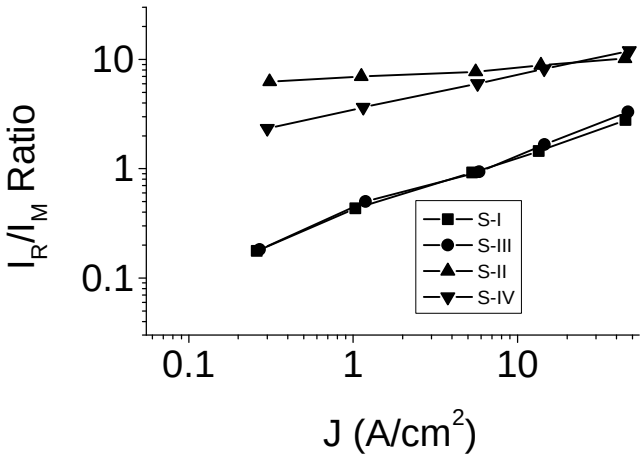

Fig. 2.20 - A comparison of I_R/I_M of diodes S-I , S-II, S-III and S-IV

The breakdown voltages of these structures have been simulated. There is no perceptible difference in the breakdown voltage of S-I, SIII and S-IV, which are more than double the breakdown voltage of S-II.

2.7 Forward '0N' Voltage

The insertion of universal contact besides resulting in improvement in reverse recovery performance is also accompanied with an improvement in forward ON voltage. This can be explained by noting that the total current flowing through the device can be expressed as

$$I = I_L + I_M + I_R = I_M \left(1 + \frac{I_L}{I_M} + \frac{I_R}{I_M}\right) \qquad (2.22)$$

Eq. (2.22) implies that an increase in I_L/ I_M or the I_R/I_M ratio would result in an overall increase in the total current flowing through the device for the same applied voltage or a decrease in forward ON voltage for the same current. A comparison of the simulated forward ON voltage of high breakdown voltage diodes is shown in Fig. 2.21. The voltage is the difference between the hole quasi-fermi voltage and electron quasi-fermi voltage in the forward ON state of different simulated diode structures at different current densities. The forward-on voltage of the diode S-II is the least amongst all the diodes at less than about 5 A/cm^2 and above 5 A/cm^2, the proposed diode S-IV is having the least forward ON voltage amongst all the four simulated diode structures.

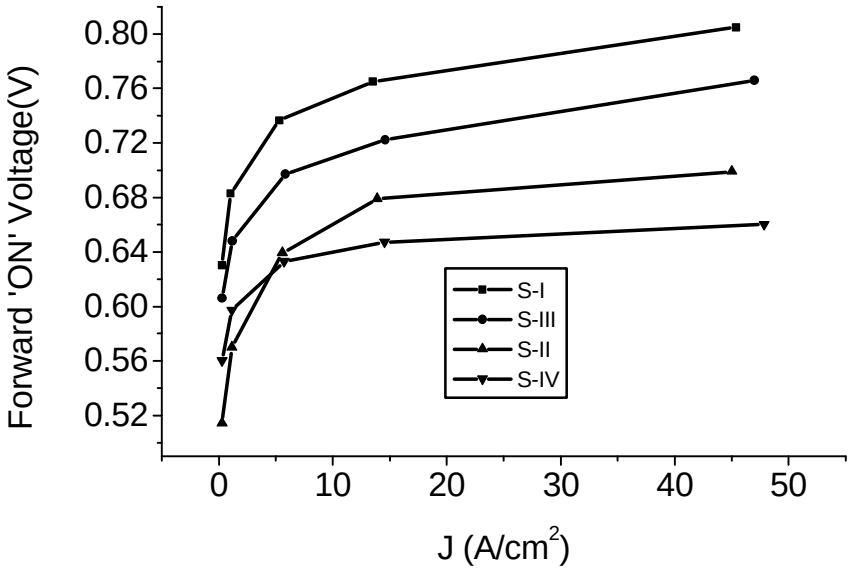

Fig. 2.21 - Forward on voltage vs current density for high voltage diode

The forward ON voltage of the diode S-III is lower by about 50 mV at 50 A/cm^2 in comparison to the conventional diode S-1. The corresponding decrease in forward ON voltage of diode S-IV is 145 mV at about 50 A/cm^2. To summarize, the incorporation of the universal contact in the p^+ region lead to improvement of switching characteristics and forward ON voltage and these improvements have been achieved without compromising the reverse blocking capability.

2.8 EXPERIMENTAL RESULTS

To verify some of the results obtained in modeling and simulation parts, diodes S-I, S-II and S-III have been fabricated. The diodes S-I and S-III have been fabricated with breakdown voltage of ~ 150 V as well of >1000V. The photograph of the breakdown voltage of low and high voltage diode is shown in Fig. 2.22 (a) and (b). The breakdown was measured at wafer level. High voltage diode could be measured up to 1000 V, though the breakdown voltage of the diode is higher than 1000V. The measured Leakage currents are given in Table 2.2.

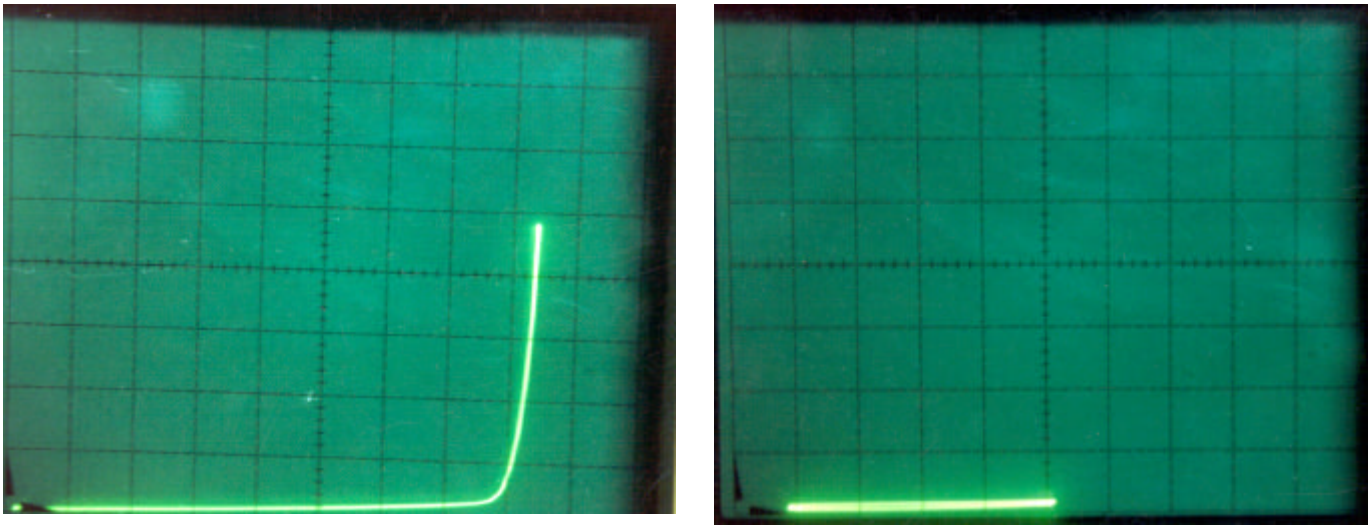

(a) (b)

Fig. 2.22 Photograph showing breakdown voltage of S-I diodes (a) Low voltage diode (Hor. Scale 20 V/Div) (b) High voltage diode (Hor. Scale 200 V/Div)

The diode S-II has also been made in the same material as of S-III but it has breakdown voltage of ~500V due to the reach-through breakdown. The technology and process flow for the fabrication of conventional and modified diodes is described in Chapter IV. The efforts have been made to keep the material and process same for these devices so as to eliminate the possibility of lifetime variation due to extraneous account. The devices have been characterized for reverse breakdown voltage, leakage current and reverse recovery. The diode physical parameters, p^+n^+ ratio and their dc characteristics are given in Table 2.2.

Table 2.2 Details of the fabricated diodes & their dc characteristics

Diode	Base Resistivity And Width	P^+ diffusion	Breakdown Voltage & leakage	n^+ diffusion in p for "universal contact" (Refer Fig.2.4)
(1)Low Voltage (S-I & S-III)	nn^+ epi, n width 15 μm & Conc.1.15 x 10^{15} /cm^3	R_s 98 Ω/sq Xj = 5.4 μm ,	BV 130-155 V Leakage 100 nA at 100V	Rs=1.8 Ω/sq, Xj= 3.2 μm (P^+:N^+ :: 20 : 20 ,20:40, 20:80 μm) in S-III
(2)High Voltage (S-I & S-III)	Bulk silicon, 210 μm , & Conc. 4 x 10^{13} /cm^3, (back n^+ diff. Sur. Conc. 1 x 10^{19} /cm^3, xj = 35 μm)	R_s 100Ω/sq, xj = 23.0 μm	BV >1000 V Leakage 5 μA at 1000V	Rs=5.6 Ω/sq, Xj= 7 μm (P^+:N^+ :: 20 : 20 ,20:40, 20:80 μm) in S-III
(3)High Voltage (S-1 & S-II)	Bulk silicon, 175 μm , Conc ~ 4 x 10^{13} /cm^3, (back n^+ diff. Sur. Conc 1 x 10^{19} /cm^3, xj = 35 μm in S-1 only)	R_s 100Ω/sq, xj = 23.0 μm	BV ~400 – 500 V Leakage 2 μA at 400V	n^+ diff., Sur. Conc. 5 x 10^{20} /cm3 , xj = 4.48 μm p+ diff. Sur. Conc 5 x 10^{19} /cm3, xj = 3.0 μm (p+ : n+ ::20 μm : 50 μm) in S- II

The experimental setup for the measurement of reverse recovery is given in Appendix 'D'. The results for reverse recovery time, measured by keeping I_F, the forward on current and I_{REV}, the reverse switching off current equal, are shown in Table 2.3. As observed from the Table 2.3, the reverse recovery is decreasing at higher current density both in S-I and S-III. Similar results were expected from the model developed and shown by the simulation experiments. The decrease in reverse recovery in low

voltage diode is around 75%, Table 2.3. The improvement in high voltage diode is 23-30%, Table 2.4. The same order of improvement was also observed during simulation. The improvement in high voltage S-II with respect to S-I is about 70%, Table 2.5. Similar results were expected from modeling and simulation. The photographs of reverse recovery waveform for S-I and S-III are shown in Fig 2.23(a) & (b) and Fig. 2.24 (a) & (b) for low and high voltage diodes respectively.

Table 2.3 - Measured reverse recovery of low voltage diodes S-I & S-III

Diode type & I.D.	Breakdown Voltage	I_F /I_{REV} (mA)	Storage time ns		Fall time ns		Reverse Recovery (τ_s + 90% of τ_f) ns		
			S-I	S-III	S-I	S-III	S-I	S-III	% Improvement
Low Voltage Diode) Base Area 0.14 x 0.14 cm^2									
S-I (1X4) Q3	155 V	10/10	1060	230	30	30	1090	260	76
		20/20	790	190	30	30	820	220	73
		30/30	680	160	30	30	710	190	73
		40/40	600	140	30	30	630	170	73
		60/60	510	110	30	30	540	140	74
		80/80	450	100	30	30	480	130	73
		90/90	425	80	30	30	455	110	76

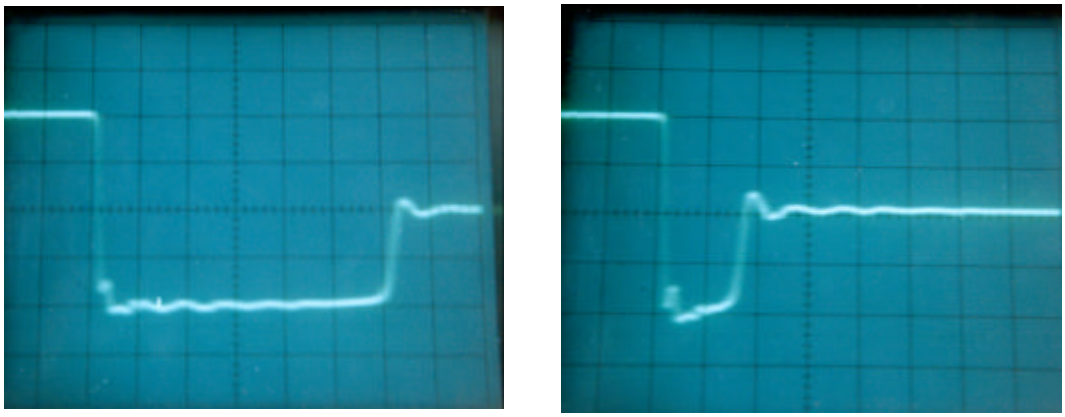

(a) **(b)**

Fig. 2.23 Photograph of reverse recovery waveform of low voltage diode (a) S-I (b) S-III (Hori. Scale 100 ns/Div, Vertical Scale 20 mA/Div)

Table 2.4 Measured reverse recovery of high voltage diode S-I & S-III

Diode type & I.D.	Breakdown Voltage	I_F/I_{REV}	Storage time µs		Fall time µs		Reverse Recovery (τ_s + 90% of τ_f) µs		
			S-I	S-III	S-I	S-III	S-I	S-III	% Improvement.
High Voltage Diode Base Area 0.1 x .1 cm^2									
S – I (R1 2X1 –Q3)	>1000 V	10/10	6	3.0	7.5	7.4	13.5	10.4	23
		20/20	4.8	2.0	7.5	7.4	12.3	9.4	23.5
		30/30	4.0	1.5	7.5	7.0	11.5	8.5	26
		40/40	3.6	1.2	7.5	6.6	11.1	7.8	30
		60/60	2.8	0.9	7.1	6.0	9.9	6.9	30
		80/80	2.4	0.8	6.8	6.0	9.2	6.8	26
		90/90	2.2	0.7	6.5	5.9	8.7	6.6	24

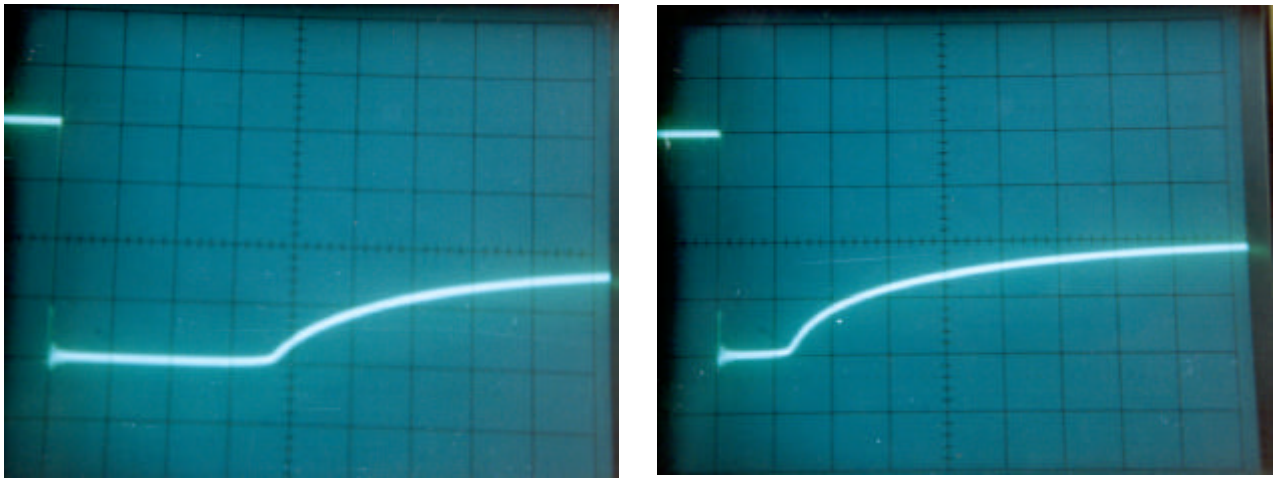

(a) **(b)**

Fig. 2.24 **Photograph of reverse recovery waveform of low voltage diode (a) S-I (b) S-III (Hori. Scale 1 ms/Div, Vertical Scale 20 mA/Div)**

Table 2.5 Measured Reverse Recovery of high voltage Diode S-I & S-II

Diode type & I.D.	Breakdown Voltage	I_F/I_{REV} (mA)	Storage time μs	Fall time μs	Reverse Recovery (τ_s + 90% of τ_f) ms	
						% Improvement.
High Voltage Diode (A comparison with Amemiya Diode)						
S – I (Device 1 X 2)	>1000 V	20/20 40/40	11.8 10.2	2.6 2.6	14.4 12.8	72 69
S - II (Device 1X2)	400-500 V	20/20	2.5 2.5	1.5 1.5	4.0 4.0	

The experimental results show an improvement of about 75% in switching performance for low voltage diodes and 23-40 % for high voltage diodes, in agreement

with the trends observed in the simulated results. The improvement in reverse recovery was accompanied by no noticeable change in the breakdown voltage.

In addition to incorporation of universal contact in the end regions, use of hetro-structures can also be potentially used to further improve the effective lifetime. By using a wide band-gap semiconductor in the middle region and suitable narrow band-gap semiconductors in the end regions, the current ratios I_L/ I_M and I_R/I_M could possibly be considerably increased leading to very low effective minority carrier lifetime in the device.

2.9 SUMMARY OF DIODE RESULTS

The use of n^+p^+ "universal contact" for improving the switching performance of power diodes was examined in detail. By incorporating the n^+p^+ "universal contact' in the end regions of a diode, an increase in the fraction of end region injected currents and significant lowering of the effective lifetime was observed. It was found that the incorporation of this modification in left region improved the reverse recovery of low voltage diodes (100 -–200 V) by 77% and for high voltage (1000 V) diode by 40%. In high voltage diodes, due to large middle region thickness, the fraction of current injected into the left region is relatively less and the improvement of reverse recovery is also less as compared to low voltage diodes. The improvement for both low and high voltage diodes was found to increase with current density, this is due to the difference in voltage dependence of current injected into the left region (ideality factor ~ 1) and the middle

region (ideality factor ~ 2). The results obtained from simulation were found to be in agreement with experimental results. A new structure incorporating universal contact in both left (p^+) and right (n^+) regions of the diode has been proposed to further improve the diode's switching performance.